

Bubbly Flow Model for Cavitating Inducer Dynamics

It is also valuable to consider the results of figures 4 to 7 of Section (Nr_q) in the context of an analytical model for the dynamics of cavitating pumps (Brennen 1978). We present here a brief physical description of that model, the essence of which is depicted schematically in figure 1, which shows a developed, cylindrical surface within the inducer. The cavitation is modeled as a bubbly mixture which extends over a fraction, ϵ , of the length, c , of each blade passage before collapsing at a point where the pressure has risen to a value which causes collapse. The mean void fraction of the bubbly mixture is denoted by α_0 . Thus far we have

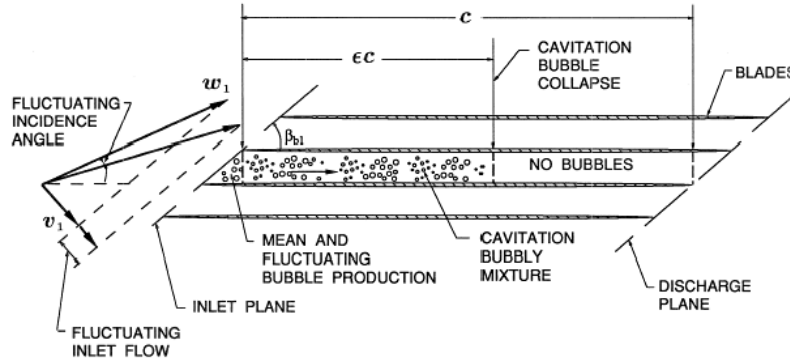


Figure 1: Schematic of the bubbly flow model for the dynamics of cavitating pumps (adapted from Brennen 1978).

described a flow which is nominally steady. We must now consider perturbing both the pressure and the flow rate at inlet, since the relation between these perturbations, and those at discharge, determine the transfer function. Pressure perturbations at inlet will cause pressure waves to travel through the bubbly mixture and this part of the process is modeled using a mixture compressibility parameter, K , to determine that wave speed. On the other hand, fluctuations in the inlet flow rate produce fluctuations in the angle of incidence which cause fluctuations in the rate of production of cavitation at inlet. These disturbances would then propagate down the blade passage as kinematic or concentration waves which travel at the mean mixture velocity. This process is modeled by a factor of proportionality, M , which relates the fluctuation in the angle of incidence to the fluctuations in the void fraction. Neither of the parameters, K or M , can be readily estimated analytically; they are, however, the two key features in the bubbly flow model. Moreover they respectively determine the cavitation compliance and the mass flow gain factor, two of the most important factors in the transfer function insofar as the prediction of instability is concerned.

The theory yields the following expressions for A_{111} , A_{112} , A_{121} and A_{122} at small dimensionless frequencies (Brennen 1978, 1982):

$$\begin{aligned}
 A_{111}\Omega &\simeq \frac{K\zeta\epsilon}{4} \left\{ \cot \beta_{b1} + \phi_1 / \sin^2 \beta_{b1} \right\} \\
 A_{112}R_{T1} &\simeq -\zeta / 4\pi \sin^2 \beta_{b1} \\
 A_{121}\Omega^2 / R_{T1} &\simeq -\pi K\zeta\epsilon / 4 \\
 A_{122}\Omega &\simeq -\frac{\zeta\epsilon}{4} \left\{ M / \phi_1 - K\phi_1 / \sin^2 \beta_{b1} \right\} \quad (\text{Nrt3})
 \end{aligned}$$

where $\zeta = \ell Z_R / R_{T1}$ where ℓ is the axial length of the inducer, and Z_R is the number of blades. Evaluation of the transfer function elements can be effected by noting that the experimental observations suggest

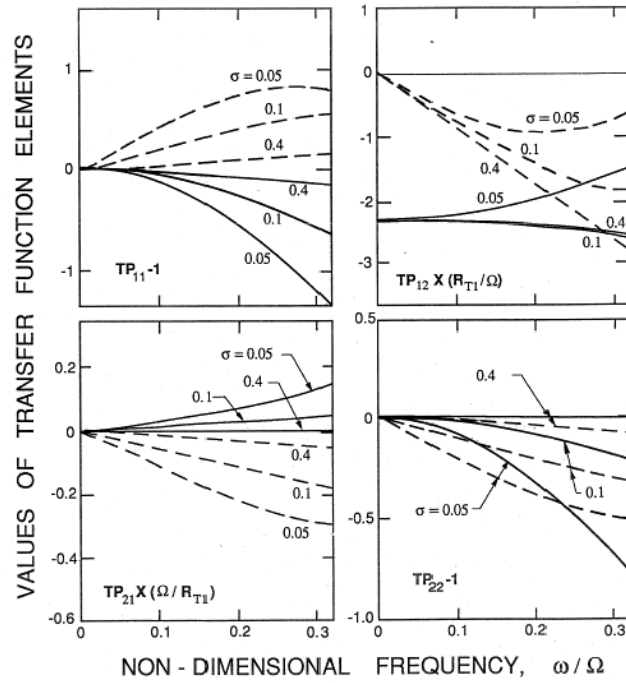


Figure 2: Transfer functions for Impellers VI and IV at $\phi_1 = 0.07$ calculated from the bubbly flow model using $K = 1.3$ and $M = 0.8$ (adapted from Brennen *et al.* 1982).

$\epsilon \approx 0.02/\sigma$. Consequently, the A_{nij} characteristics from equations (Nrt3) can be plotted against cavitation number. Typical results are shown in figures 4 to 7 of Section(Nrq) for various choices of the two undetermined parameters K and M . The inertance, A_{112} , which is shown in figure 4 of Section (Nrq), is independent of K and M . The calculated value of the inertance for these impellers is about 9.2; the actual value may be somewhat larger because of three-dimensional geometric effects that were not included in the calculation (Brennen *et al.* 1982). The parameter M only occurs in A_{122} , and it appears from figure 6 of Section (Nrq) as though values of this parameter in the range $0.8 \rightarrow 0.95$ provide the best agreement with the data. Also, a value of $K \approx 1.3$ seems to generate a good match with the data of figures 5, 6 and 7 of Section(Nrq).

Finally, since $K = 1.3$ and $M = 0.8$ seem appropriate values for these impellers, we reproduce in figure 2 the complete theoretical transfer functions for various cavitation numbers. These should be directly compared with the transfer functions of figure 3 of Section (Nrq). Note that the general features of the transfer functions, and their variation with cavitation number, are reproduced by the model. The most notable discrepancy is in the real part of TP_{21} ; this parameter is, however, usually rather unimportant in determining the stability of a hydraulic system. Most important from the point of view of stability predictions, the cavitation compliance and mass flow gain factor components of the transfer function are satisfactorily modeled.